arXiv:cond-mat/0504645v1 [cond-mat.supr-con] 25 Apr 2005

Field-enhanced critical parameters in magnetically nanostructured superconductors

M. V. Milošević and F. M. Peeters

Departement Fysica, Universiteit Antwerpen (Campus Drie Eiken), Universiteitsplein 1, B-2610 Antwerpen, Belgium

PACS. 74.78.-w – Superconducting films and low-dimensional structures.
PACS. 74.25.Dw – Superconductivity phase diagrams.
PACS. 74.25.Op – Mixed states, critical fields, and surface sheaths.
PACS. 74.25.Qt – Vortex lattices, flux pinning, flux creep.

Abstract. – Within the phenomenological Ginzburg-Landau theory, we demonstrate the *enhancement* of superconductivity in a superconducting film, when nanostructured by a lattice of magnetic particles. Arrays of out-of-plane magnetized dots (MDs) extend the critical magnetic field and critical current the sample can sustain, due to the interaction of the vortex-antivortex pairs and surrounding supercurrents induced by the dots and the external flux lines. Depending on the stability of the vortex-antivortex lattice, a peak in the $H_{ext} - T$ boundary is found for applied integer and rational matching fields, which agrees with recent experiments [Lange *et al.* Phys. Rev. Lett. **90**, 197006 (2003)]. Due to compensation of MDs- and H_{ext}-induced currents, we predict the field-shifted $j_c - H_{ext}$ characteristics, as was actually realized in previous experiment but not commented on [Morgan and Ketterson, Phys. Rev. Lett. **80**, 3614 (1998)].

Introduction. – Arrays of nanoscale ferromagnetic (FM) particles are potential devices for applying well-defined local magnetic fields. When such a nano-engineered magnetic lattice is combined with a superconducting (SC) film, various new phenomena occur. Only recently, submicrometer lithographic techniques have been developed that allow to reduce the size of magnetic inclusions to a scale comparable with the characteristic lengths of conventional superconductors [1]. Because of its technological relevance, flux pinning in these FM/SC heterostructures has been the subject of a vast amount of theoretical and experimental work (see [2–4] and references therein). Introducing magnetic dot lattices has proven to be a very useful tool to understand the plethora of physical effects related to the interactions between vortices and material imperfections, including matching effects or collective locking of the flux lattice to the magnetic dot array, with consequently higher critical current [5].

Over the last years, the interest shifted towards the more fundamental properties of magnetically textured superconductors. For example, though often neglected, the stray field of the particles may strongly modulate the order parameter in the underlying superconductor. Recently [6], the appearance of various vortex-antivortex states was predicted. Lange *et al.* [7] demonstrated experimentally that if such sample is exposed to an additional homogeneous field, the superconductivity in some parts of the sample is enhanced, due to

© EDP Sciences

field-compensation effects. Moreover, in certain parameter-range, one can even restore superconductivity by *adding* magnetic field. Besides FM/SC structures, only (EuSn)Mo_6S_8, organic λ-$(BETS)_2FeCl_4$ materials and $HoMo_6S_8$ show this unconventional behavior [8].

Theoretical formalism. – The present Letter puts emphasis on the interplay of the magnetic fields in a thin SC film with a square array of submicron magnetic dots (MDs) with perpendicular magnetization (see Fig. 1), exposed to a background homogeneous field (in our earlier works [6] no external magnetic field was present). The superconductor and the magnetic array are only magnetically coupled, as a thin oxide layer is assumed between them to prevent the proximity effect. We investigate the influence of the magnetization/stray field of the MDs on the critical parameters of the superconductor. We present the first theoretical (quantitative) explanation of the magnetic-field-induced superconductivity. We broaden this physical picture and show how the critical current in these samples can also be nanoengineered by inducing additional currents in the sample by carefully perpetrated MD-arrays.

In our theoretical treatment of this system, we use the non-linear Ginzburg-Landau (GL) formalism, combined with specific boundary conditions. The energy difference between the superconducting and the normal state, in units of $H_c^2/4\pi$, can be expressed as

$$\Delta\mathcal{G} = \int \left[-|\Psi|^2 + \frac{1}{2}|\Psi|^4 + \frac{1}{2}|(-i\nabla - \mathbf{A})\Psi|^2 + \kappa^2(\mathbf{H} - \mathbf{H}_0)^2 \right] dV, \tag{1}$$

where $\mathbf{H}_0$ denotes the total magnetic field imposed on the superconductor (magnetic dots plus external field). Minimization of Eq. (1) leads to two coupled GL equations which we solve following a numerical approach proposed by Schweigert *et al.* (see Ref. [9]) on a uniform Cartesian grid with typically 10 points/ξ in each direction. In the present case, we took for the simulation region a rectangle $W_x \times W_y$, where $W_x = W_y = 16W$ (W is the period of the MD lattice). In order to include periodicity of SC and MD lattice in our calculation, we apply the periodic boundary conditions [10], with specific gauge transformations given in Ref. [6].

To explore the superconducting state, we start from randomly generated initial configurations, increase/decrease the magnetization of the MDs or change the value of the applied external field, and let the vortex-configuration-solution relax to a steady-state one. In addition, we always recalculate the vortex structure starting from the Meissner state ($\Psi = 1$) or the normal state ($\Psi \approx 0$) as initial condition. By comparing the energies of all found vortex

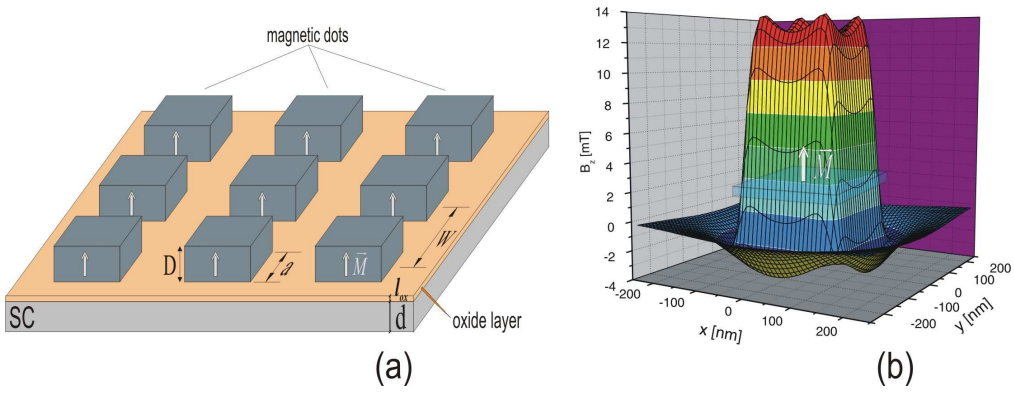

Fig. 1 – (a) The superconducting film underneath a regular array of square magnetic dots with out-of-plane magnetization. (b) The magnetic field profile under a Co dot with $a = 200$nm and $D = 20$nm.

states we determine the ground state configuration. In this Letter, we are mostly interested in the critical parameters for the superconducting/normal (S/N) transition. In our calculations, the criterion $|\psi|^2_{max} < 10^{-5}$ denotes the normal state.

The field-enhanced critical field. – Recently, Lange *et al.* [7] demonstrated experimentally the field-induced-superconductivity (FIS) effect. A lattice of out-of-plane magnetic dots is placed on top of a SC film (see Fig. 1). The magnetic stray field of each dot has a positive z-direction under the dots and a negative one in the area between the dots. The basic idea is straightforward: added to a homogeneous magnetic field H_{ext}, these dipole fields *enhance* the z-component of the effective magnetic field in the small area just under the dots and reduce the total field everywhere else in the SC film (i.e. enhance superconductivity). The sample consisted of a 85nm-thick Pb film, covered by a 10nm Ge layer for protection from oxidation and proximity effect. The square magnetic dots (side length about 0.8μm) were made as Pd(3.5nm)/[Co(0.4nm)/Pd(1.4nm)]$_{10}$ multilayers, and arranged in a square array with period 1.5μm. Knowing values of these parameters, we can apply our numerical approach to the investigated system. In Fig. 2 the calculated $H_{ext} - T$ diagram is shown for positively magnetized dots. The temperature is introduced in our calculation through the temperature dependence of the coherence length $\xi(T) = \xi(0)/\sqrt{1 - T/T_c}$. The best agreement between the experimental and theoretical $H_{ext} - T$ diagrams was obtained for $\xi(0) \approx 28$nm and magnetization value of $M = 3.32 \times 10^5$A/m. While the magnetization corresponds to expected values (between the Co and Pd values), the coherence length we found is smaller than the known values for Pb films of 35-40nm. However, ξ is hardly a controllable quantity, and strongly depends on the preparation of the sample. Notice that because of the so-called

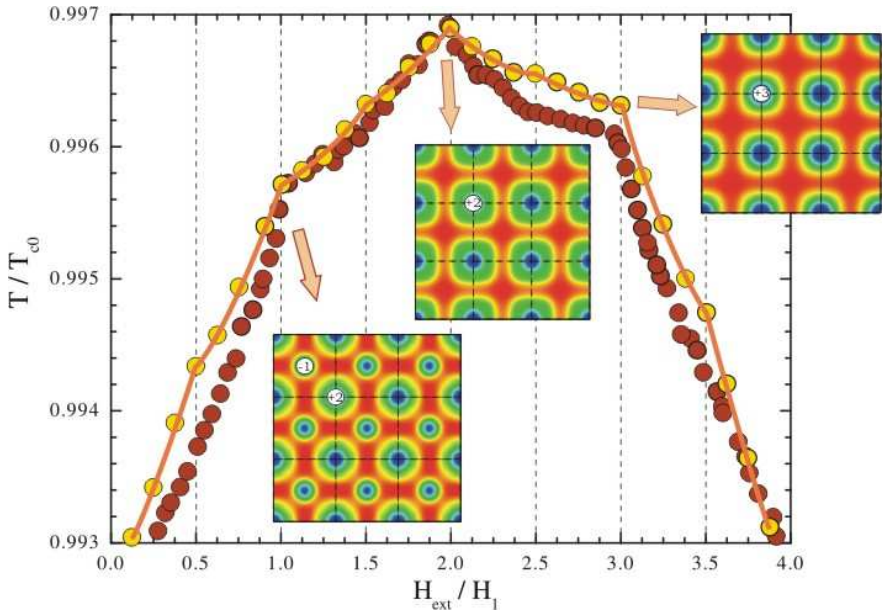

Fig. 2 – The $H_{ext} - T$ diagram: red dots give the experimental data of Ref. [7], and the yellow ones correspond to the theoretical results. The Cooper-pair density insets (blue/red color - low/high density) illustrate the vortex configurations for the applied first and third matching field (taken deeper inside the SC state). T_{c0} denotes the critical temperature in the absence of any magnetic field.

"virial theorem" [10], our approach works only for integer number of external flux lines per simulation cell. In this particular case, we used a 4×4 supercell, so we were able to calculate the phase boundary only in points described by $H_{ext} = \frac{n}{16} H_1$, where n is an integer number.

The H_{ext}-T phase boundary is clearly altered by the presence of the magnetic dot array. Contrary to a conventional symmetric (with respect to $H_{ext} = 0$) S/N phase boundary, the H_{ext}-T boundary for the magnetically textured SC is strongly asymmetric, as shown in Fig. 2. The maximal critical temperature was found for the second matching field $H_{ext} = 2H_1$ when $M > 0$ ($H_1 = 9.2$G is the first matching field, where number of vortices in the system matches the number of magnetic pinning centers). The H_{ext}-T phase diagram is shifted over $\Delta H_{ext} = 2H_1$ but at the same time is not symmetric with respect to $H_{ext} = 2H_1$. Due to this applied-field-shift, the positive critical magnetic field of the superconductor at given temperature is *enhanced* by magnetic nanostructuring. However, note that the superconductivity becomes less immune to the negative applied fields. If needed, that can be accommodated by changing the polarity of the MDs, resulting in the opposite field-shift effect.

Lange *et al.* estimated the negative flux (of the MD stray field) between the magnetic dots to $\Phi^- \approx 2.1\Phi_0$ per unit cell. From the field compensation effect described above, one expects the maximal critical temperature when external flux matches the flux of the negative stray field of the dots, which is indeed the case in Fig. 2. However, this effect is not related to the field-compensation, but to compensation of induced currents in the sample, mostly through vortex-antivortex annihilation. We found the same qualitative behavior for a range of magnetization values of the dots, corresponding to the negative flux range $\Phi^-/\Phi_0 = 2.21 - 3.22$ (maximal $T_{S/N}$ found for $H_{ext} = 2H_1$), while the best quantitative agreement with experimental data was found for $\Phi^- = 2.8\Phi_0$. In this range of magnetization, each magnetic dot creates a $L = 2$ giant vortex under each dot and two antivortices at each interstitial site [6]. Obviously, for the applied second matching field, the external flux lines annihilate with the interstitial antivortices, decreasing the total number of (anti)vortices in the sample and giving rise to the critical temperature (see insets of Fig. 2). Similar phenomenon happens for the first and third matching field. For $H_{ext} = H_1$, one antivortex and one external vortex annihilate, leaving one antivortex per unit cell at the central interstitial position. This configuration is very stable and leads to an increase of T_c. On the other hand, for $H_{ext} = H_3$, the two antivortices annihilate with two external vortices, and the third external flux line is pinned by the magnetic dot, leading to a giant vortex with vorticity $L = 3$ at each pinning site. Therefore, temperature fluctuations affect this vortex configuration much less than the one for $H_{ext} = H_1$ due to absence of weakly pinned interstitial (anti)vortices. As a consequence, asymmetry in the $H_{ext} - T$ boundary with respect to the second matching field is observed.

In addition, one should notice the fine structure in the $H-T$ boundary around the so-called rational applied magnetic fields. Namely, we found small kinks in the phase boundary for external fields $H_{i/2}$, where $i = 1,\ 3,\ 5,\ 7$ (see Fig. 2). For these fields, the number of external flux lines does not correspond to an integer multiple of the number of antivortices present in the sample. Therefore, after a very selective annihilation, fractional vortex-antivortex configurations with positive net vorticity per unit cell are formed. The Cooper-pair density plots of such configurations are shown in Fig. 3. The newly formed vortex-antivortex lattices are still able to preserve the symmetry, and due to the strong pinning of such a lattice, an enhancement of superconductivity is observed. Note that the unit cell of the vortex configurations for half-matching fields is of size 2x2 lattice cells, which is different from the matching field cases (see insets in Fig. 2). Note also that each state shown in Fig. 3 exhibits certain peculiarity: in (a) interstitial sites are alternately occupied by 1 or 2 antivortices; in (b) giant vortex ($L = 2$) under each dot is clearly deformed due to its attraction with antivortices at every other interstitial site; in (c) there are no antivortices present, and magnetic dots alternately

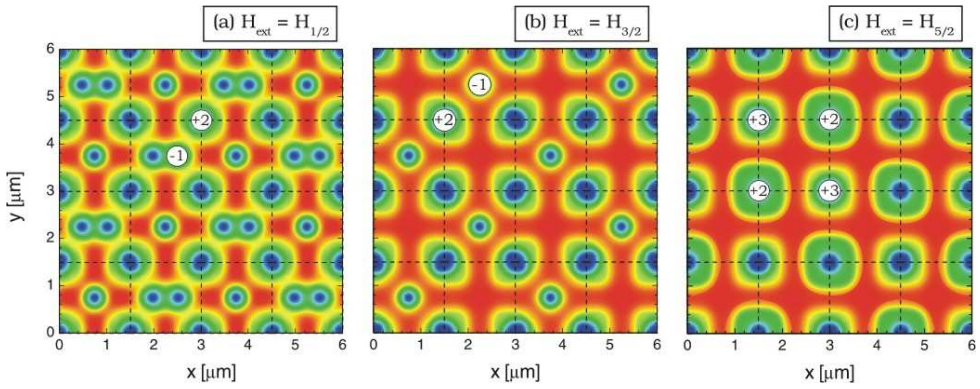

Fig. 3 – The Cooper-pair density contourplots for the fractional vortex-antivortex lattices with positive net vorticity, obtained for rational applied field: (a) $H_{ext} = H_{1/2}$, (b) $H_{ext} = H_{3/2}$, and (c) $H_{ext} = H_{5/2}$. Thin lines indicate the unit cells of the magnetic dot lattice.

capture 2 or 3 vortices in the form of a giant vortex. However, the realization of fractional states is rather difficult, as they are sensitive to the fluctuations in the applied field (and other parameters determining competing interactions). For that reason, theoretically found kinks in the S/N boundary are hardly visible in the experimental data. However, for well defined applied fields, we expect that these novel vortex-antivortex states with non-zero total vorticity are observable using e.g. scanning probe techniques like Hall and Magnetic Force Microscopy.

The field-shifted critical current characteristics. – Magnetic nanostructuring of superconductors influences not only their critical field but critical current as well. It is well known that magnetic lattice on top of a SC film pins the external flux lines when M and H_{ext} have the same polarity [4, 5]. According to Refs. [4, 5], this results in a reduced vortex mobility and consequently enhanced critical current, with the maximal current for $H_{ext} = 0$. While this behavior is found for *weak* magnetic pinning centers, more complicated physical picture is expected for stronger ones. To investigate this, we exposed our (Pb) sample with $a = 200$nm, $D = 20$nm, $W = 800$nm and given magnetization M and temperature $T/T_c = 0.9$ to a gradually changed homogeneous magnetic field, starting each time from the normal state. Then the current is applied in the x-direction through $A_{cx} = const.$ (now $A_0 = A_{md} + A_{ext} + A_c$) which does not interfere with our boundary conditions, and the resulting current in the system is calculated. When the critical value of A_{cx} is reached, the motion of (anti)vortices can no longer be prevented and superconductivity is destroyed. The results of our calculations for the critical current j_c as a function of the applied field are shown in Fig. 4(a) for different values of the MD-magnetization. For small magnetization (open dots) an asymmetry in the $j_c(H_{ext})$ dependence with respect to $H_{ext} = 0$ is observed. This confirms the findings of Refs. [4, 5], and indicates vortex pinning for parallel orientation of the applied field and the magnetic moments. For negative applied field, antivortices are introduced in the system which are repelled by the magnetic dots. They are weakly pinned at interstitial sites, further suppressing superconductivity and easily stimulated to motion, leading to lower j_c.

However, for higher M we found a field-offset in the $j_c(H_{ext})$ characteristics. For $M =$ 510G and $M = 1400$G (bulk Ni and Co values), the maximal j_c peak was found for $H_{ext} = H_1$ and $H_{ext} = H_2$, respectively. Intuitively, and according to our findings in previous section, we know that if we increase M, vortex-antivortex (VAV) pairs nucleate. When positive homogeneous field is applied, external flux lines annihilate with the interstitial antivortices, and a

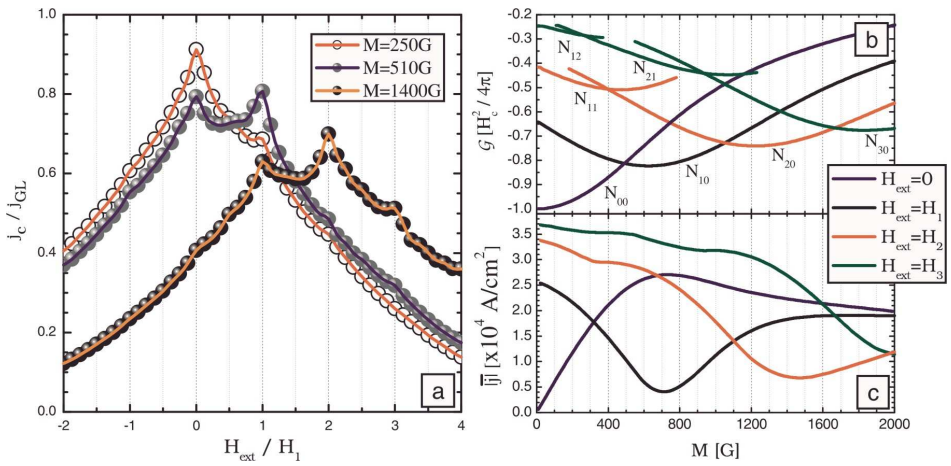

Fig. 4 – (a) Critical current (in units of Ginzburg-Landau current j_{GL}) versus the applied magnetic field in units of the first matching field. (b) The Gibbs free energy and (c) the spatial average of the current magnitude in the sample, as a function of the magnetization of the magnetic dot array ($a = 200$nm, $D = 20$nm, $W = 800$nm, above the Pb film at $T/T_c = 0.90$).

maximal critical current is obtained for a magnetic field such that all antivortices are annihilated. In such a case, the field-offset in the $j_c(H_{ext})$ curve indicates the number of VAV-pairs per magnet. However, this mechanism is not always realized. The free energy diagram in Fig. 4(b) (blue curve) shows that there are no vortex-antivortex pairs induced in the sample, even for high M. Namely, vortices and antivortices cannot be adequately separated since the magnetic lattice is too dense compared to ξ(T) [6]. Nevertheless, when external field is applied, the equilibrium vortex configurations (denoted by N_{ab}, with a-number of pinned vortices per dot, b-number of interstitial vortices) can have *lower* energy than the superconducting state in the absence of the applied field. This phenomenon occurs due to the current compensation effect, between the magnet-induced antivortex-like currents and the currents of external vortices, when pinned by the magnets. This feature is obvious from Fig. 4(c), where average magnitude of current in the sample is shown as function of the magnet strength and applied field. Note that the ground state crossings in Fig. 4(b) do not directly correspond to the lowest current values in Fig. 4(c), due to the energy contribution of the Cooper-pairs distribution. Overall, one concludes that the total current in the sample for given parameters is the determining factor for the field-shift in the $j_c(H_{ext})$ characteristics.

Interestingly enough, the phenomenon of the field-shift of the critical current was experimentally observed in Ref. [5], but not commented on. Namely, the authors were concerned only about the field-polarity-dependent pinning, and overlooked this issue. For comparison, we performed the calculations for a SC film with a triangular MD-lattice on top, where the parameters are taken from Ref. [5] [array of Ni dots ($R_d = 120$nm, $D = 110$nm, $W = 0.6\mu$m) covered by a Nb film ($d = 95$nm), with $T_c \approx 8.60 \pm 0.10$K]. Fig. 5 shows the critical current in the sample as a function of an applied field, at temperatures $T/T_c \approx 0.965$, 0.97, and 0.98 (orange lines) compared to experimental data at $T = 8.40$, 8.46, and $T = 8.52$K, respectively. As clearly shown in Fig. 5(b), the maximum in the critical current shifts to the first matching field when approaching T_c. In Fig. 4(c), we demonstrated the compensation of vortex-currents with M-dependent magnet-induced currents. In the present case, for fixed magnetization M, the vortex-currents profile is changed by temperature (which effectively changes $\xi(T)$).

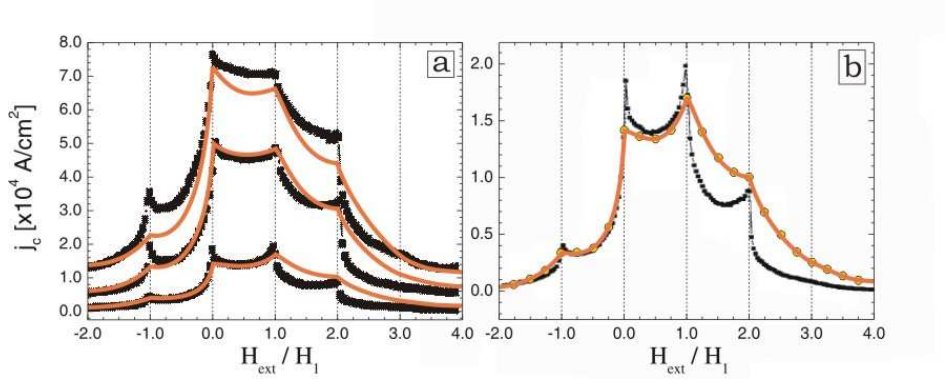

Fig. 5 – Critical current versus the applied magnetic field in units of the first matching field ($H_1 = 57.5$G), for parameters taken from Ref. [5] (a) for temperatures $T/T_c = 0.965$, 0.970, and 0.980 (top to bottom); (b) enlargement of the $T/T_c = 0.980$ data. Yellow dots (and/or orange lines) denote the theoretical results. Experimental data are from Ref. [5].

Our theoretical results, denoted by orange lines in Fig. 5, confirm the field-shift found experimentally. This fit was obtained for $\xi(0) = 36$nm and $\lambda(0) = 90$nm values, with $M = 625$G, 20% larger than the saturation magnetization of bulk Ni (510G). From H_{c2} measurements, the mean free path was estimated in Ref. [5] as $l \approx 5$nm (dirty limit), which justifies the low $\xi(0)$ obtained theoretically. Besides the agreement in the field shift in the critical current dependence and the qualitative agreement, one should notice the discrepancy in the critical current values. In our opinion, the smearing of the matching peaks in our results is caused by the large coherence length at temperatures close to T_c. $\xi(T)$ becomes comparable to the distance between the magnets, leading to overlapping vortices. On one hand, this leads to enhanced current-compensation effects, crucial for the field-shifted $j_c(H_{ext})$ characteristics. However, this overlap results in less effective matching effects (both integer and rational). Also, one should note the partial 'washing-out' of the magnetic alignment when sweeping applied magnetic field in the experiment. This leads to a less ordered vortex structure for non-matching fields, effectively decreasing the critical current (i.e. pronouncing peaks at matching fields). Despite these differences, the experiment-theory agreement is apparent, demonstrating that the predicted field-shift of the maximum of the critical current is not sensitive neither to the geometry of the magnetic lattice nor to the shape of the magnetic dots (Fig. 4 vs. Fig. 5).

In conclusion, we have shown that magnetic nanostructuring of the SC film not only enhances its critical field in a controlled fashion, but also can enhance the maximal current the sample can sustain. Moreover, the magnetic field for which the maximal critical current is achieved can also be engineered. Our findings are in excellent agreement with existing experiments [5, 7]. We interpret experimental results and our predictions through the interaction of the external flux lines with the magnet-induced currents (and vortex-antivortex pairs) in the SC. These interactions may lead to novel vortex-antivortex lattices with positive net vorticity.

Acknowledgements. – The authors acknowledge D. Vodolazov, V. Moshchalkov and M. Van Bael for valuable discussions. This work was supported by the Flemish Science Foundation (FWO-Vl), the Belgian Science Policy, and the University of Antwerp (GOA).

REFERENCES

[1] J.I. Martin *et al.*, *Phys. Rev. Lett.*, **79** (1997) 1929.
[2] C. Reichhardt, C.J. Olson, and F. Nori, *Phys. Rev. B*, **57** (1998) 7937.
[3] J.I. Martin *et al.*, *Phys. Rev. Lett.*, **83** (1999) 1022.
[4] M.J. Van Bael *et al.*, *Phys. Rev. B*, **59** (1999) 14674.
[5] D.J. Morgan and J.B. Ketterson, *Phys. Rev. Lett.*, **80** (1998) 3614.
[6] M.V. Milošević and F.M. Peeters, *Phys. Rev. Lett.*, **93** (2004) 267006; *ibid. Phys. Rev. B*, **68** (2003) 024509; D.J. Priour, Jr. and H.A. Fertig, *Phys. Rev. Lett.*, **93** (2004) 057003.
[7] M. Lange *et al.*, *Phys. Rev. Lett.*, **90** (2003) 197006.
[8] H. W. Meul *et al.*, *Phys. Rev. Lett.*, **53** (1984) 497; M. Giroud *et al.*, *J. Low Temp. Phys.*, **69** (1987) 419; S. Uji *et al.*, *Nature (London)*, **410** (2001) 908.
[9] V.A. Schweigert, F.M. Peeters, and P.S. Deo, *Phys. Rev. Lett.*, **81** (1998) 2783.
[10] M.M. Doria, J.E. Gubernatis, and D. Rainer, *Phys. Rev. B*, **39** (1989) 9573.